Air dielectric barrier discharges plasma surface treatment of three-dimensional braided carbon fiber reinforced epoxy composites

Hao Li, Hui Liang, Fang He, Yuan Huang, Yizao Wan *

School of Materials Science and Engineering, Tianjin University, Tianjin 300072, China

ARTICLE INFO

ABSTRACT

The deposition of coatings on the surface of three-dimensional braided carbon fiber reinforced epoxy (C_{3D}/EP) composites will be helpful to their applications. However, they are unsuitable to be deposited due to their low surface free energies, poor wettabilities and poor adhesions. Since treatment of polymers or composites by non-thermal plasmas is a fast, versatile and environmentally friendly surface modification technique, the plasma treatment of C_{3D}/EP composites is investigated in this paper. Dielectric barrier discharges (DBD) in ambient air are used. C_{3D}/EP (V_f=36%) samples with thickness of 2 mm are placed into the plasma configuration. Time for plasma treatment is 30 s, 60 s and 120 s. The chemical and physical changes induced by the treatments on C_{3D}/EP surface are examined using contact angle measurements, X-ray photoelectron spectroscopy (XPS) and atomic force microscopy (AFM). The water advancing contact angles of the plasma-treated C_{3D}/EP samples change from 98.6° for the untreated sample to the lower value 45.7° after plasma treatment of 30 s and 42.7° of 120 s. XPS results reveal that the composites modified with the DBD at an atmospheric pressure show a significant increase in oxygen-containing and nitrogen-containing groups, such as C–O, O–C=O and NO_2. The AFM images of the untreated and plasma-treated C_{3D}/EP samples show that the composites surfaces roughen. The roughness of the untreated C_{3D}/EP is 1.6 nm, while after plasma treatment of 30 s, 60 s and 120 s the values are 2.4 nm, 3.0 nm and 3.9 nm respectively. These results demonstrate that the surfaces of the C_{3D}/EP samples are more active, hydrophilic and rough after plasma treatments using a DBD operating in ambient air.

© 2008 Elsevier B.V. All rights reserved.

1. Introduction

Fiber reinforced polymer composites have been used widely in aerospace, marine and automobile industries during the past few decades (1960 onwards) due to their good engineering properties such as high specific strength and stiffness, lower density, high fatigue endurance, high damping and low thermal coefficient (in fiber direction), etc [1]. Three-dimensional braided carbon fiber reinforced epoxy (C_{3D}/EP) composites are excellent materials for surgery or aviation because of their good properties, such as improved overall performance, high strength, desirable modulus, splendid friction and wear characteristics, etc [2,3]. The deposition of some coatings on the surface of C_{3D}/EP composites will be greatly helpful to their applications. However, C_{3D}/EP composites are unsuitable to be deposited due to their low surface free energies, poor wettabilities and poor adhesions. As a result, surface modification of C_{3D}/EP composites is quite required. Treatment of polymers or composites by non-thermal plasmas has become more and more popular as a surface modification technique, since it is a fast, versatile and environmentally friendly method [4].

Application of plasma technologies in fiber reinforced composites is mainly focus on cleaning and roughening of fibers in order to enhance the fiber-matrix adhesion [4–6], treatment of the fracture surface as a means for exposing filler particles in the fracture surface [7,8] or treatment of membranes [9]. There are comparatively a few studies on the plasma surface treatment of the thick composite materials [10]. Zhang [11] studied the tribological behavior of the argon plasma-treated carbon fiber reinforced PEEK composites. Meyer [5] carried out surface etching of three dimensional shaped parts of carbon fiber reinforced epoxy and PEEK composites by plasma etching with an O_2 and C_2F_6 mixture. Kim et al. [6,12] investigated the surface of carbon/epoxy layers of prepregs by examining the strength of single lap composite adhesive joint after argon plasma or oxygen plasma treatment. Kyong [13] inspected the peel strength and the shear strength of aluminum/CFRP composites in which the surface of the aluminum was treated using DC plasma and the surface of the CFRP was treated by Ar^+ ion assisted reaction method under oxygen environment. However, there are few reports of atmospheric pressure air dielectric barrier discharges (DBD) plasma treatment of fiber reinforced polymer composites surfaces even if this treatment is more economical than other plasma treatments because it need no special gas and subsequent special equipments. Otherwise, morphology of three-dimensional braided composites surfaces after polishing is different to normal composites. Therefore, it is necessary to investigate the atmospheric pressure air DBD plasma treatment of three-dimensional braided fiber reinforced polymer composites surfaces.

* Corresponding author. Tel./fax: +86 22 27405056.
  E-mail address: yzwantju@yahoo.com (Y.Z. Wan).

The atmospheric pressure air DBD plasma treatment of C_{3D}/EP composites is investigated in this paper and the chemical and physical changes induced by the treatments on C_{3D}/EP surface are examined using contact angle measurements, X-ray photoelectron spectroscopy (XPS) and atomic force microscopy (AFM).

2. Materials and methods

2.1. Materials and surface treatment

The samples were C_{3D}/EP composites prepared through RTM (resin transfer molding) process. The concentration of carbon fiber was 36 vol.% and that of epoxy resin was 64 vol.%. Samples were of the thickness of 2 mm and rectangular shape. They have been mechanically polished up to obtain a mirror-like surface and then cleaned by ultrasonic wave for 30 min.

The atmospheric pressure plasma treatments were performed using a DBD operating in air. Two circular copper electrodes (diameter = 150 mm) were placed in the DBD plasma configuration. Each electrode was covered with a quartz glass plate with thickness of 2 mm and circular area of 210 mm diameter. The gas gap between the two quartz glass plates was 6 mm. Before starting the experiments, samples were placed on the lower quartz glass plate.

The pulsed types AC power supply presented voltage whose voltage was 8 kV and frequency was 8 kHz. The discharge current was 40 mA and peak pulse current was 300 mA. When discharged, a large number of dense filamentary microdischarges generated from upper electrode and bombarded the surface of samples. Time for plasma treatment was 30 s, 60 s and 120 s.

2.2. Contact angle measurements

Surface wettability and hydrophilicity of the C_{3D}/EP sample were investigated by advancing and receding contact angle measurements. Contact angles were obtained using a DCAT21 contact angle measuring device (Dataphysics company—Germany). Distilled water was used as test liquids.

2.3. X-ray photoelectron spectroscopy (XPS)

XPS analysis was used to determine the chemical changes on the C_{3D}/EP surfaces introduced by plasma treatment. XPS measurements were carried out on a PHI-1600 X-ray Photoelectron Spectroscope (PE company—USA) operated at 250 W. The non-monochromatic Mg K_α X-ray radiation (hv = 1486.6 eV) was used for excitation. The working pressure in the analyzing chamber was in the range of 10^{-8}–10^{-9} Torr. Correction of the energy shift due to the static charging of the samples was accomplished with the C1s peak at 284.6 eV as a reference.

2.4. Atomic force microscopy (AFM)

AFM images were obtained by a Nanoscope IIIa atomic force microscope (DI company—USA). The surface topology and the root mean square (RMS) roughness were recorded and analyzed.

3. Results and discussion

3.1. Contact angle measurements

The advancing/receding contact angle measurement method, which quantifies hysteresis, is especially suited for understanding the surface wettability and controlling the surface wetting behavior [14]. Table 1 indicates the effects of discharge time on contact angles against water. With time for treatment prolongs, it is observed that advancing angle of C_{3D}/EP sample is on the decrease, especially in the first 30 s. It changes from 98.56° for the untreated sample to the lower value 45.65° after

Table 1
Contact angle of C_{3D}/EP surfaces untreated and after plasma treatment for multiple times

Time for plasma treatment (s)	Contact angle of C_{3D}/EP surfaces		
	Advancing angle (deg)	Receding angle (deg)	Contact angle hysteresis (deg)
0	98.56	20.26	78.30
30	45.65	13.49	32.16
60	43.73	21.98	21.75
120	42.73	22.04	20.69

plasma treatment of 30 s. After 60 s and 120 s discharges, the advancing angles reduce to 43.73° and 42.73° respectively. So it can be seen that saturation of the surface modification reaches after 30 s exposure.

It is known that the advancing contact angle is less sensitive to surface roughness and heterogeneity than the receding angle and therefore commonly used to calculate surface and interfacial tension components, which are vital to indicate surface wettability and hydrophilicity [15]. Table 1 shows that advancing contact angles of C_{3D}/EP surface reduce with treatment time increasing, which reveal that surface wettability and hydrophilicity of C_{3D}/EP surface are enhanced with treatment time increasing. This can be explained by the changes of surface topology and chemical compositions (see Sections 3.2 and 3.3).

As can be seen in Table 1, the receding angle of the untreated C_{3D}/EP surface (20.26°) reduces to 13.49° after 30 s plasma treatment and then raises to 21.98° and 22.04° respectively after 60 s and 120 s discharges.

The advancing contact angle is more sensitive to the hydrophobic component while the receding angle is more sensitive to the hydrophilic one if the surface is made up of heterogeneous components [14]. The difference between the advancing and receding contact angles is known as the contact angle hysteresis [16].

Table 1 shows the contact angle hysteresis of C_{3D}/EP surfaces. The contact angle hysteresis of the plasma-treated C_{3D}/EP sample changes from 78.30° for the untreated sample to 32.16° after plasma treatment of 30 s. After 60 s and 120 s discharges, the contact angle hysteresis are 21.75° and 20.69° respectively.

Contact angle hysteresis has been attributed to solid surface roughness, surface heterogeneity, and some other surface chemical properties [17–21]. But surface roughness is not expected to result in contact angle hysteresis for surfaces with roughness at the nano-scale level [14,17]. A number of studies [18–20] have reported that surface chemical heterogeneities, surface swelling, penetration of liquid into the solid surface, and surface reorientation of chemical functional groups can all lead to contact angle hysteresis. In this paper, C_{3D}/EP surface is made up of two regularly interlaced areas. They are epoxy, whose concentration is 64% or more, and exposed carbon fiber areas. When plasma treated, C_{3D}/EP surface, including epoxy and carbon fiber areas, is more active and rough with time for treatment prolongs (see Sections 3.2 and 3.3). These can reduce heterogeneity of carbon fiber and epoxy on the surfaces of composites because exposed carbon fiber areas, which are less hydrophilic than epoxy originally, become more active and meanwhile the epoxy areas, which are less rough than carbon fiber areas originally, become rougher. The reduction of surface heterogeneity is one of the reasons of contact angle hysteresis decreasing. Otherwise, Gong [21] found that PVA-p-PDAmC10 LB film has a very large contact angle hysteresis (>80°), which means that reorientation of the surface configuration takes place dramatically, and the hysteresis can be greatly reduced (<30°) by UV-irradiation due to the photocycloaddition in the side chains of PVA-p-PDAmC10. Because of the similar contact angle hysteresis results, reorientation of C_{3D}/EP surface is under suspicion of decreasing after plasma treatment and becoming another reason of contact angle hysteresis reducing.

3.2. XPS analysis

XPS survey spectra of untreated and plasma treated C_{3D}/EP surfaces show similar photoelectron peaks attributed to C, O and N.

Table 2
Concentration of the different elements of the C_{3D}/EP surfaces untreated and after plasma treatment for multiple times

Time for plasma treatment (s)	Concentration of the different elements of the C_{3D}/EP surfaces (%)		
	C1s	O1s	N1s
0	73.1	25.9	1.0
30	64.3	34.6	1.1
60	59.0	39.8	1.2
120	60.4	37.6	2.0

The concentration of these elements is given in Table 2. In the first 60 s, the carbon concentration reduces whereas oxygen concentration increases markedly and nitrogen concentration increases lightly with increasing time for treatment. From 60 s to 120 s, carbon concentration increases lightly whereas oxygen concentration decreases but nitrogen concentration increases observably from 1.2 to 2.0. The atomic elemental composition yields an O/C ratio of 0.35 in the case of untreated sample and 0.54, 0.67 and 0.62 when C_{3D}/EP are exposed to air plasma for 30 s, 60 s and 120 s. It can be seen that the first 30 s exposure is the most important period of the surface activation.

The XPS results reveal the strong oxidation level at the surface of air plasma exposed C_{3D}/EP. The presence of air in the plasma enhances oxygen bonding at the surface. The increase in hydrophilic chemical compositions (e.g. oxygen containing substances) and the decrease in hydrophobic ones (e.g. containing carbon organic substance) are easily seen from Table 3. This is similar to that of some other surfaces treated by plasma in presence of oxygen [22–25].

As can be seen in Fig. 1, the C1s spectrum of the untreated or plasma treated C_{3D}/EP surface can be decomposed into three components: a component at 284.6 eV due to the C–C bonds, a component at 286.7 eV due to C–O bonds and a component at 289.0 eV due to the O–C=O bonds [26]. The concentration of the C–C, C–O and O–C=O groups of the untreated and plasma-treated C_{3D}/EP surface is shown in Table 3. With increasing time for treatment, the C–C concentration reduces whereas C–O and O–C=O concentrations increase. From 30 s to 60 s, C–O concentrations show no increase but O–C=O concentration increases observably from 13.5 to 15.2.

When plasma is employed on the C_{3D}/EP surface, the surface and the molecules are exposed to high reactive regime of DBD. It can generate a wide range of active species including atomic oxygen, ozone, nitrogen oxides, neutral molecules, radicals and ultraviolet radiation. The main reactive species responsible for oxygen inclusion is atomic oxygen formed in the discharge because of the dissociation of O_2 molecules by electron impact [27–29]. Thus after plasma treatment, the C_{3D}/EP surface is active and hydrophilic.

Fig. 2 shows the N1s spectra of the C_{3D}/EP surfaces untreated and after plasma treatment for multiple times. It is found that besides the changing of contents of C–N/N–H bonds (~400.0 eV) [30–32], the NO_2 or ONO_2 groups (~407.5 eV) [32–34] appear with increasing time for treatment, especially after 60 and 120 s treated. Although more polar NO_2 or ONO_2 groups also increase the surface energy and result in a

Table 3
Concentration of the different carbon-containing groups of the C_{3D}/EP surfaces untreated and after plasma treatment for multiple times

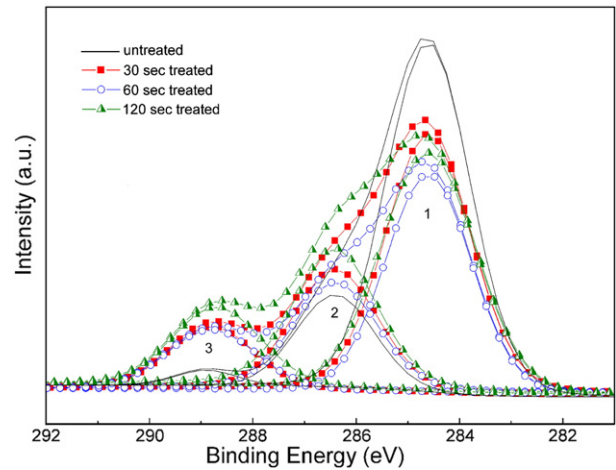| Time for plasma treatment (s)	Concentration of the different carbon-containing groups of the C_{3D}/EP surfaces (%)		
	C–C (284.6 eV)	C–O (286.7 eV)	O=C–O (289.0 eV)
0	76.2	21.5	2.3
30	58.6	27.9	13.5
60	56.9	27.9	15.2
120	50.5	33.2	16.3

Fig. 1. C1s spectra of the C_{3D}/EP surfaces untreated and after plasma treatment for multiple times. (1. C–C, 2. C–O, 3. O=C–O).

lower contact angle, which contribute to the absorption of nitrogen free atoms from the plasma air [35], their role in surface mechanisms in this study is little because nitrogen content is much too low, as can be seen in Table 2.

3.3. AFM images

When C_{3D}/EP samples exposed to plasma, not only chemical but also physical changes happen on their surfaces. Fig. 3 shows three-dimension topology of C_{3D}/EP surfaces untreated and after plasma treatment for multiple times. The untreated surface is flat. After plasma treated, there are some prominent parts on the surface and the number and uniformity of the prominent parts increase with treatment time increasing. These cause surface roughness changing, which is described in Table 4. The root mean square (RMS) roughness of the untreated C_{3D}/EP is 1.6 nm, while after plasma treatment of 30 s, 60 s and 120 s the values are 2.4 nm, 3.0 nm and 3.9 nm respectively.

These results are similar to the results of an increasing average roughness on polyethylene films after plasma treatment in helium/nitrogen mixtures at atmospheric pressure [36] and an increasing roughness on PET films after DBD treatment in air at atmospheric
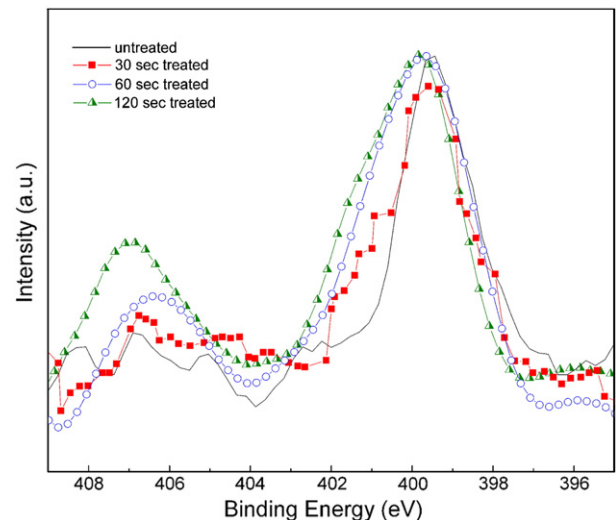

Fig. 2. N1s spectra of the C_{3D}/EP surfaces untreated and after plasma treatment for multiple times.
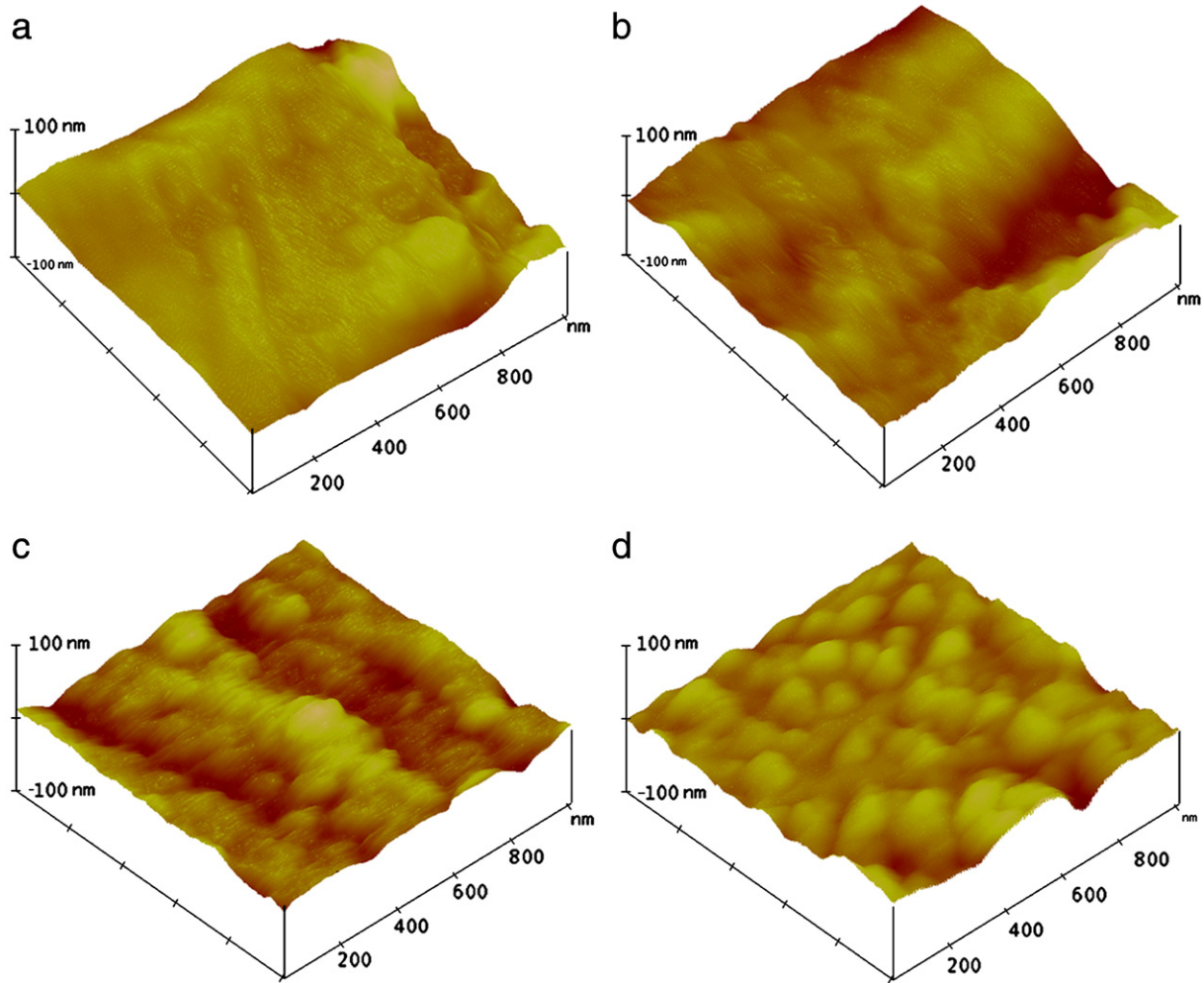
Fig. 3. AFM images of the C_{3D}/EP surfaces untreated and after plasma treatment for multiple times. (a. Untreated, b. 30 s treated, c. 60 s treated, d. 120 s treated).

pressure [37]. The discharge may preferential physical etch amorphous regions. On the untreated surface the grains or crystallites could be hidden by the outermost amorphous regions. After etching of the amorphous low cohesion surface layer the grains or crystallites become visible and contaminants, oligomers and amorphous layers existing on the surface are removed. The etching of the amorphous regions may continue by a migration of free radicals and provide an increase in size of the grains after treatment. The nucleation might be actually initiated on the surface electrical active sites created by DBD exposure, which act as attractors for the propagation of grains and crystallites existing on the surface. The defaults inherently present on the substrate may act as nucleation centers leading to the peaks and grains formation [36,38]. In this study, the difference in crystallinity of sample components and preferential ablation of one of the components might be important, too. Plasma etching removes the unstable compositions on sample surface to make it rougher. So it can be concluded that proper plasma treatment will roughen surface of both polymers and polymer matrix composites.

This roughening also leads to the decrease of advancing contact angles of C_{3D}/EP surface, as discussed in Section 3.1.

4. Conclusion

In this paper, the chemical and physical modifications of atmospheric pressure plasma-treated C_{3D}/EP composites are studied. The plasma treatments are performed using a DBD operating in air. It is shown that plasma treatment leads to a significant decrease in water advancing contact angle and contact angle hysteresis of C_{3D}/EP surface. XPS measurements show an evident increase in oxygen-containing and nitrogen-containing functional groups on the C_{3D}/EP surface, such as C–O, O–C=O and NO_2. AFM images of composite surface modified with the DBD at atmospheric pressure show that air DBD plasma treatment roughen C_{3D}/EP surfaces and the roughness increase with treatment time increasing. The results indicate that C_{3D}/EP sample surfaces are more active, hydrophilic and rough after plasma treatments using a DBD operating in ambient air provide. These will be greatly helpful to the deposition of some coatings on the surface of this kind of composites and then expand their applications.

Table 4
RMS roughness of the C_{3D}/EP surfaces untreated and after plasma treatment for multiple times

Time for plasma treatment (s)	RMS roughness of the C_{3D}/EP surfaces (nm)
0	1.6
30	2.4
60	3.0
120	3.9

References

[1] S.P. Sandeep, K. Tarun, M.D. Yogesh, Compos. Struct. 84 (2008) 114.
[2] Y.Z. Wan, Y.L. Wang, Y. Huang, F.G. Zhou, B.M. He, G.C. Chen, et al., Compos. Sci. Technol. 65 (2005) 1237.
[3] Y.Z. Wan, G.C. Chen, S. Raman, J.Y. Xin, Q.Y. Li, Y. Huang, Wear 260 (2006) 933.
[4] M. Meyer, A. Mittasch, G. Staudigl, R. Suchentrunk, Surf. Coat. Technol. 59 (1993) 297.
[5] R.Z. Li, L. Ye, Y.W. Mai, Composites Part A 28A (1997) 73.
[6] J.K. Kim, D.G. Lee, Compos. Struct. 57 (2002) 37.
[7] V. Khunova, J. Hurst, I. Janigova, V. Smatko, Polym. Test. 18 (1999) 501.
[8] I. Janigova, V. Khunova, J. Kozankova, Polym. Test. 18 (1999) 51.
[9] R.C. Ruaan, T.H. Wu, S.H. Chen, J.Y. Lai, J. Membr. Sci. 138 (1998) 213.
[10] K. Haruna, H. Hamada, Z. Maekawa, J. Adhes. Sci. Technol. 10 (1996) 1089.
[11] R. Zhang, A.M. Haeger, K. Friedrich, Q. Song, Q. Dong, Wear 181–183 (1995) 613.
[12] M.H. Kim, K.Y. Rhee, J.H. Kim, D.H. Jung, Mater. Sci. Eng., A 448 (2007) 269.
[13] K.Y. Rhee, J.H. Yang, Compos. Sci. Technol. 63 (2003) 33.
[14] C. Emil, Adv. Colloid Interface Sci. 133 (2007) 51.
[15] D.Y. Kwok, A. Leung, C.N.C. Lam, A. Li, R. Wu, A.W. Neumann, J. Colloid. Interface Sci. 206 (1998) 44.
[16] C.N.C. Lam, R. Wu, D. Li, M.L. Hair, A.W. Neumann, Adv. Colloid Interface Sci. 96 (2002) 169.
[17] R.E. Johnson, R.H. Dettre, in: E. Matijevic (Ed.), Surface and Colloid Science, Wiley-Interscience, New York, 1969, p. 85.
[18] R.J. Good, in: K.L. Mittal (Ed.), Contact Angle, Wettability and Adhesion, VSP, 1993, p. 3.
[19] R.D. Hazlett, in: K.L. Mittal (Ed.), Contact Angle, Wettability and Adhesion, VSP, 1993, p. 173.
[20] A. Marmur, Colloid. Surf., A 136 (1998) 209.
[21] Y.K. Gong, F. Nakanishi, K. Abe, Mol. Cryst. Liq. Cryst. Sci. Technol., Sect. A 327 (1999) 123.
[22] C.Q. Wang, X.N. He, Appl. Surf. Sci. 253 (2006) 926.
[23] N.D. Geyter, R. Morent, C. Leys, L. Gengembre, E. Payen, S.V. Vlierberghe, et al., Surf. Coat. Technol. 202 (2008) 3000.
[24] R. Morent, N.D. Geyter, C. Leys, L. Gengembre, E. Payen, Surf. Coat. Technol. 201 (2007) 7847.
[25] N. Danish, M.K. Garg, R.S. Rane, P.B. Jhala, S.K. Nema, Appl. Surf. Sci. 253 (2007) 6915.
[26] D. Briggs, M.P. Seah, Practical Surface Analysis Volume 1: Auger and X-ray Photo-electron Spectroscopy, John Wiley and Sons, Chichester, 1990.
[27] U. Kogelschatz, Plasma Chem. Plasma Process 23 (2003) 1.
[28] Z. Fang, Y. Qiu, E. Kuffel, J. Phys., D Appl. Phys. 37 (2004) 2261.
[29] Z. Fang, Y. Qiu, Y. Luo, J. Phys., D Appl. Phys. 36 (2003) 2980.
[30] F. Darinka, O. Alenka, C.B. Sonja, J. Mater. Process. Technol. 209 (2009) 584.
[31] Z.Y. Xiao, Y.C. Liu, J.Y. Zhang, D.X. Zhao, Y.M. Lu, D.Z. Shen, et al., Semicond. Sci. Technol. 20 (2005) 796.
[32] C.L. Perkins, S.H. Lee, X.N. Li, S.E. Asher, T.J. Coutts, J. Appl. Phys. 97 (2005) 034907.
[33] J. Torres, C.C. Perry, S.J. Bransfield, D.H. Fairbrother, J. Phys. Chem., B 107 (2003) 5558.
[34] A. Tanaka, R. Oiwa, K. Yoshihara, J. Surf. Sci. Soc. Jpn. 20 (11) (1999) 791.
[35] W.J. Liu, Y.C. Lan, Y.C. Chen, W.C. Lo, C.H. Lin, Surf. Coat. Technol. 201 (2007) 6530.
[36] G. Borcia, A. Chiper, I. Rusu, Plasma Sources Sci. Technol. 15 (2006) 849.
[37] P. Esena, C. Riccardi, S. Zanini, M. Tontini, G. Poletti, F. Orsini, Surf. Coat. Technol. 200 (2005) 664.
[38] G. Borcia, N. Dumitrascu, G. Popa, Surf. Coat. Technol. 197 (2005) 316.